Solid Earth Discuss., doi:10.5194/se-2017-17, 2017
Manuscript under review for journal Solid Earth
Discussion started: 22 March 2017

Solid Earth Discussions

Mantle roots of the Emeishan plume: an evaluation based on telesismic P-wave tomography

Chuansong He[1*], M. Santosh[2, 3]

[1]*Institute of Geophysics, China Earthquake Administration, Beijing 100081, China*

[2]*Centre for Tectonics, Resources and Exploration, Department of Earth Sciences, University of Adelaide, SA 5005, Australia*

[3]*School of Earth Sciences and Resources, China University of Geosciences Beijing, 29 Xueyuan Road, Beijing 100083, China*

Abstract: The voluminous magmatism associated with Large Igneous Provinces (LIP) is commonly correlated to upwelling plumes from the Mantle Transition Zone or the Core-Mantle Boundary (CMB). Here we analyse seismic tomographic data from the Emeishan LIP in southwestern China. Our results reveal vestiges of delaminated crustal and (or) lithospheric material in the cental part of the study area, and upwelling mantle in the southern part. Our results do not provide any conclusive evidence for upwelling mantle plume rooted in the CMB beneath the Emeishan LIP. We therefore suggest that the magmatism and the Emeishan LIP formation might be connected with the melting of delaminated lower crustal and (or) lithospheric components and associated plume-like upwelling from the mantle transition zone.

Key word: Emeishan Large Igneous Province; Teleseismic P-wave tomography;

* Corresponding author. Tel.: 86-10-68729303; Fax: 86-10-83534760.
Email address: hechuansong@aliyun.com

Solid Earth Discuss., doi:10.5194/se-2017-17, 2017
Manuscript under review for journal Solid Earth
Discussion started: 22 March 2017

Lithospheric and (or) delamination; Mantle plume; Tectonics.

1. Introduction

The large-scale and transient magmatic events on the globe at different times during Earth history are closely linked to mantle dynamics (Coffin and Eldholm, 2001; Ernst and Buchan, 2001). The punctuated but intense magmatic activities over the globe has generated several Large Igneous Provinces (LIPs) in different regions (Uenzelmann-Neben, 2013; Pirajno and Hoatson, 2012). Mantle plumes which are upwellings of hot material from deeper parts of the Earth (Arndt, 2000) have been invoked to explain the link between LIP and modern volcanoes. LIPs are characterized by large lava outpourings, such as those found in Siberia, India, and Emeishan, which also have important implications in surface environmental changes including mass extinctions (Buiter, 2014; Wignall, 2011).

Mantle upwellings received attention when Wilson (1963) suggested that the Hawaiian Islands were produced when oceanic lithosphere moved over a stationary 'hot spot' in the mantle, following which the role of plumes and their relation to mantle convection was further realized (Morgan, 1971). It is now widely recognized that upwelling mantle plumes generate many LIPs and numerous small chains of seamounts (Griffiths and Campbell, 1990; Hofmann, 1997; Maruyama et al., 2007; Safonova et al., 2009; White, 2010; Dobretsov, 2011, Safonova and Santosh, 2014). When upwelling mantle plume impinges on continental or oceanic lithosphere, large-scale eruption and

Solid Earth Discuss., doi:10.5194/se-2017-17, 2017
Manuscript under review for journal Solid Earth
Discussion started: 22 March 2017

intrusion of mafic and ultramafic melts occur generating LIPs (Coffin and Eldhom, 1992, Pirajno, 2007; Sheth, 2007b; Bryan and Ernst, 2008; Shellnutt and Iizuka, 2012).

The basaltic rocks of LIPs have been investigated to understand the source, nature and tectonic setting of LIPs formation (Smith and Asimow, 2005; Herzberg and Asimow, 2008; Shellnutt and Iizuka, 2012). The Emeishan basalts (ca. 257 - 262 Ma) in southwest China are exposed over an area of 0.25-0.3 million square kilometers in the Sichuan, Yunnan and Guizhou provinces comprising a total volume of about 0.25 million km^3 (Huang and Opdyke, 1998), with thickness of the basaltic flow ranging from one to two hundred meters in the eastern part to more than five kilometers in the west (Ali et al., 2010; Deng et al., 2010). The Emeishan LIP hosts some of the world-class Fe–Ti–V oxide and Ni–Cu sulfide deposits (Pang et al., 2013; Zhou et al., 2013). The region has been divided into three zones (inner, intermediate and outer) (Fig. 1) based on biostratigraphic, sedimentological and geochemical characteristics (Xu et al., 2001; Deng et al., 2010).

Previous studies suggested the Emeishan flood basalts with mantle plume impingement at the base of the lithosphere causing large-scale regional up-doming prior to volcanism (Shellnutt et al., 2012; Shellnutt, 2013, 2014; Li et al., 2002; Gao et al., 1999; Liu et al., 2008) with a short eruption period of less than 1 Ma (Song et al. 2004). However, the primary evidence for upwelling mantle plume has remained elusive. Some workers (e.g. Ukstins Peate and Bryan, 2008) have also challenged the concept of

Solid Earth Discuss., doi:10.5194/se-2017-17, 2017
Manuscript under review for journal Solid Earth
Discussion started: 22 March 2017

upwelling mantle plume leading to LIP formation in the Emeishan area. It has also been argued that that submarine volcanism took place during emplacement of the Emeishan LIP and that some lava flows close to the centre of the LIP were erupted in a submarine setting (Ukstins Peate and Bryan, 2008; Ali et al., 2010). This model considers that the products of initial eruption were extruded at or around sea level, and that the moderately positive topography is a reflection of the rapid accumulation of the volcanic pile (Peate and Bryan, 2008). Therefore, in order to further understand the Emeishan LIP formation, it is necessary to investigate the deep structure or mantle dynamics beneath the Eemishan LIP area.

In the past two decades, seismic tomography has increasingly found application as a potential tool to explore the heterogeneous structure of the Earth's interior, which in turn is important to gain insights into mantle dynamics and crust-mantle interaction processes. Several seismic tomographic studies have been carried out on the Emeishan LIP and surrounding regions, including 2.5 dimensional tomography of the uppermost mantle (Lü et al., 2014), ambient noise Love and Rayleigh wave tomography (Li et al., 2010, 2009), teleseismic P-wave tomography (Yang et al., 2014; Huang et al., 2015; Bai et al., 2011), local earthquake tomography (Huang et al., 2009; Xu et al., 2012), interstation Pg and Sg differential traveltime tomography (Li et al., 2014) and Pn anisotropic tomography (Lei et al., 2014). Generally, most of these studies targeted the crustal and upper mantle velocity structure in this area.

Solid Earth Discuss., doi:10.5194/se-2017-17, 2017
Manuscript under review for journal Solid Earth
Discussion started: 22 March 2017

In this study, we carried out a systematic tomographic analyses with a view to construct the velocity structure or mantle dynamics of the upper mantle beneath the Emeishan LIP area. The results provide a vivid image of the upwelling mantle and the lower crustal and (or) lithospheric delamination. Our results further demonstrate the dynamic relationship between delamination and upwelling mantle.

2. Data and method

The basic principle for teleseismic tomography assumes that the relative travel-time residuals resulted from the heterogeneity in the model space (e.g. Yang et al., 2014; Zhao et al., 1992). The location of the seismic ray crosses through the boundary of the study region was determined by a 1D velocity model and theoretical travel time and seismic ray paths are obtained by the fast raytracing technique (Zhao et al., 1992, Yang et al., 2014). 3D grids are employed to express the velocity perturbation values, and any point in the model space can be calculated from values of the surrounding eight nodes by linear interpolation (Zhao et al., 1992, 1994, 1997, 2009; 2002, 2013; Zhao and Lei, 2004; Zhao and Ohtani, 2009;, Zhao, 2001, 2004).

In this study, we collected data recorded by China seismic network from July 2007 to March 2014 which comprises 228 seismic stations in the study region (Fig. 1, Fig. 2). The 371 seismic events were selected with epicentral distance ranging from 30°-85°correspond to earthquake magnitude >6.0. *P* arrivals were correlated on the vertical component after bandpass filtering between 0.3 and 3 Hz. Our assembled data set

Solid Earth Discuss., doi:10.5194/se-2017-17, 2017
Manuscript under review for journal Solid Earth
Discussion started: 22 March 2017

contains 42500 *P*-wave arrivals. Based on the distribution of the relative arrival time, we limited the relative arrival time of >-2s and <2s used to tomographic inversion (Fig. 3). To analysize this data set, we used the tomographic method of Zhao et al (1994). The three-dimension grid nodes was set up. The lateral grid spacing is $1^\circ \times 1^\circ$ and the vertical grid spacing are 50, 100, 200, 300, 400, 500, 600, 700 and 800 km respectively. After the crustal correction to remove the effect of lateral crustal heterogeneity (crustal correction depth: 50 km) (Jiang et al., 2015), the velocity perturbations from the one-dimensional iasp91 Earth model (Kennett and Engdahl, 1991) at each grid node was taken as unknown parameter. The LSQR algorithm (Paige and Saunders, 1982) was used to solve the large and sparse system of observation equations with damping and smoothing regularizations (Zhao, 2004). The optimal value of the damping is based on the trade-off curve between the RMS travel-time residuals and the norm of the model, after many tests, and eventually, 15 were adopted as damping parameter (Fig. 4).

The results from tomographic inversion should be assessed along with resolution and error analyses. The procedure to evaluate the resolution of a tomographic result is to first calculate a set of travel time delays which result from tracing the actual rays through a synthetic test structure, followed by the inversion of the delays as though they are data, and finally comparing the synthetic inversion result with the initial structure (Zhao et al., 1992). Following this method, the synthesized data were inverted to evalute whether the assigned checkerboard pattern could be recovered or not. Here, we designed the lateral grid spacing as $1^\circ \times 1^\circ$ and the vertical grid spacings are 50, 100, 200, 300, 400, 500

Solid Earth Discuss., doi:10.5194/se-2017-17, 2017
Manuscript under review for journal Solid Earth
Discussion started: 22 March 2017

600, 700 and 800 km. Positive and negative velocity perturbations of 5% were assigned to all the 3-D grid nodes. The results show that the resolution is generally high in most parts of the study area (Fig. 5), except for the marginal region and 50 and 800 km depth sections. We also carried out the checkboard test along west-east profiles (Fig. 1, Fig. 6), all results show high resolution at all profile and the synthetic data can be recovered at main part, except for western part of the section, the north-south profiles also show high resolution at most part, except for the marginal region (Fig. 7). The results of the checkboard test demonstrated our data and calculation adequately meet with the required resolution for this study.

3. Results

The results from this study show large-scale high velocity perturbation at 50,100, 200, and 300 km depth sections in the northeastern part of the study area or Yangtze block which reflects the lithospheric root of the Sichuan Basin (Fig. 8). This result is consistent with previous teleseismic P-wave tomographic studies (Yang et al., 2014; Huang et al., 2015; Li et al., 2006; Bao et al., 2009). A recent receiver function study indicates large-scale delamination at the central and southern parts of this area (He et al., 2014), which might have triggered large-scale mantle convection leading to the high velocity domain in this region. Therefore, tomographic images show a large-scale high velocity perturbation at 300 and 400km depth at the central part (Fig. 8, Hv1) which may be associated with the crustal and (or) lithospheric delamination. Huang et al. (2015) also defined a large-scale high velocity perturbation at 350 and 400 km depth, which is

Solid Earth Discuss., doi:10.5194/se-2017-17, 2017
Manuscript under review for journal Solid Earth
Discussion started: 22 March 2017

consistent with our results. High velocity perturbations are also revealed at 500, 600 and 700 km depth sections (most in the mantle transition zone) (Fig. 8, Hv2), which might connect with the crustal and (or) lithospheric delamination or vestiges of subduction slab of the Indian plate (Yang et al., 2014). In the southern part of the study area, large-scale low velocity perturbations are seen at 50, 100, 200 and 300 km depth section (Fig. 8 Lv1). Furthermore, these low velocity perturbations broadly overlap at different depths, possibly indicating a connection with the upwelling mantle. Huang et al. (2015) and Yang et al. (2014) also defined a low velocity perturbation at 100-200 km depth, which is also consistent with our results. In the 700 and 800 km depth sections, there is an obvious low velocity perturbation in the southern part of the region, which might represent the vestige of the upwelling mantle.

In the west-east direction profile (Fig. 9), the high velocity perturbation at the root of Sichuan basin can be clearly seen in Figs. 9a and b. The large-scale high velocity occurs in the upper mantle region around 26-28°, which is consistent with the results from 300 and 400 km depth sections (Fig. 8), which further suggests large-scale delamination process beneath the Emeishan LIP area. Several discontinuous high velocity perturbations are seen in the mantle transition zone, possibly related to crustal and (or) lithospheric material delaminated into the mantle transition zone. Alternately, these features might also correspond to the vestiges of the subduction slab of the Indian plate. In Fig. 9d, there is a large-scale low velocity perturbation in the upper mantle (along the 24°N), which reflect upwelling mantle originating from the mantle transition zone. Yang et

Solid Earth Discuss., doi:10.5194/se-2017-17, 2017
Manuscript under review for journal Solid Earth
Discussion started: 22 March 2017

al. (2014) and Huang et al. (2015) also defined a low velocity perturbation or upwelling mantle almost at the same location (along the 25°N).

In order to further evaluate our results, we took 4 profiles along the north-south direction (Fig. 10). In Fig. 10e, there is a low velocity perturbation or large-scale upwelling mantle, which is consistent with Lv1. In Fig 10f and h, there is a low velocity perturbation or upwelling mantle originating from the mantle transition zone. In Fig. 10g, the upwelling mantle may originate from the mantle transition zone, because the low velocity perturbation is very weak at the lower mantle part, which might also be due to the low resolution of the profile (Fig. 7).

The tomographic image identified by this study shows an obvious low velocity perturbation in the upper mantle beneath the southern part of the study area, there are no vestiges of any upwelling mantle plume beneath the Emeishan LIP. In contrast, there are the low velocity perturbation in the upper mantle and mantle transition zone, we speculate that the low velocity perturbation in the southern part of the region (Fig. 8, Fig. 9 and Fig. 10) might be associated with crustal and (or) lithospheric delamination. These vestiges are also identified within high resolution checkboard test (please see Fig. 5, Fig. 6 and Fig. 7), confirming that our results are reliable.

4. Discussion

Solid Earth Discuss., doi:10.5194/se-2017-17, 2017
Manuscript under review for journal Solid Earth
Discussion started: 22 March 2017

4.1 The location of the Emeishan LIP formation

The south China block docked with the Indochina Block on the southwest in the Triassic along the Ailaoshan-Song Ma suture, on the west along the Longmenshan Fault, and on the north with the North China Craton along the Qinling–Tongbai–Hong'an–Dabie–Sulu orogenic belt (Li et al., 2002; Zhou and Zhu, 1993; Mao et al., 2013; Zheng et al., 2013). The Emeishan LIP is considered to have formed in the Permian-Triassic (Song et al., 2013; Chung and Jahn, 1995), suggesting a close link with the tectonics associated with the block amalgamation. The LIP was broken up by the Red River Fault (Xiao et al., 2004) and is now bounded by the Longmenshan fault (He et al., 2007). However, the ~260-Ma Emeishan LIP in SW China and northern Vietnam includes voluminous continental flood basalts that are believed to have formed from same upwelling mantle (Chung and Jahn, 1995; Xu et al., 2004; Zhou et al., 2006; Wang et al., 2007). Recent studies also suggested that tectonic lenses of the same basaltic sequence (Camthuy Formation) and associated rocks are present in northern Vietnam (Tien, 2000; Shi and Shen, 1998), and were displaced several hundred kilometers to the southeast by Oligo-Miocene sinistral motion along the Ailao Shan-Red River Fault (Ali et al., 2005), suggesting that the Emeishan LIP was formed after the closure of the south China block and the Indochina Block. Although the paleogeographic location of the region of the LIP is near the equator in the early Permian (Ali et al., 2005; Enkin et al., 1992), the Emeishan terrane arrived in the present location in the later Permian or early Triassic prior to the LIP formation.

Recent receiver function study also demonstrated a convective circulation system

Solid Earth Discuss., doi:10.5194/se-2017-17, 2017
Manuscript under review for journal Solid Earth
Discussion started: 22 March 2017

between the lower crust and the upper mantle transition zone beneath the Emeishan area associated with the Emeishan LIP formation (He et al., 2014), which further suggests the formation of the Emeishan LIP at the present location.

4.2 The mechanism of the Emeishan LIP formation

Predictions based on numerical and fluid dynamic modelling show that mantle plumes originating from either the MTZ or the CMB would result in broad domal uplift (>1,000km wide, 500 to >1,000m high) preceding volcanism in LIPs (Peate and Bryan, 2008; Campbell and Griffiths, 1990; Richards et al., 1989). However, the location and distribution of the voluminous mafic volcaniclastic deposits, pillow lavas and marine sediments in the Emeishan LIP do not confirm with the zonal definition of a broad uplifted dome (Peate and Bryan, 2008). Therefore, the relationship between dynamic uplift and plume-related process in the Emeishan LIP has remained equivocal (Peate and Bryan, 2008; Sheth, 2007a; Ali et al., 2010; Shellnutt, 2014).

The rise and impingement of mantle plumes on continental and oceanic lithospheric plates would lead to the formation of mafic/ultramafic lower crust (Pirajno, 2007). Although, some of the previous studies indicated a high velocity lower crust beneath the Emeishan LIP (Xu et al., 2007), suggesting mafic/ultramafic lower crust generated by lower crustal underplating or the upwelling mantle plume during later Permian (Shellnutt, 2014; Zhong et al., 2009; Xu et al., 2004; Tang et al., 2015; Usuki et al., 2015). However, the dominantly felsic to intermediate lower crust in this area identified from receiver function analyses (He et al., 2014, 2009) do not favour any large-scale underplating in

Solid Earth Discuss., doi:10.5194/se-2017-17, 2017
Manuscript under review for journal Solid Earth
Discussion started: 22 March 2017

the Emeishan LIP area (He et al., 2014; S.S. Sun et al., 2012).

Alternate models consider that the LIP magmatism was triggered by decompression-induced melting of upper mantle beneath zones of lithospheric extension or fractures (Uenzelmann-Neben, 2013) which does not require any upwelling mantle plume. Pre-eruptive subsidence and asthenospheric flow into voids created by delamination of dense eclogitic lower crust and (or) lithosphere have been proposed by some workers (Anderson, 2007; Hales et al., 2005), such as in the case of the Siberian trap basalts (Elkins-Tanton and Hager, 2000).

Tomography studies have indicated a high velocity perturbation zone at 500 and 600 km depth section identified by this study and the earlier studies in the Emeishan LIP area (Ferris et al., 2003; Yang et al., 2014). This might link the cold material detached or delaminated from the lower crust and (or) lithosphere into the upper mantle leading to the velocity increase.

The crustal and (or) lithospheric delamination can generate mantle upwelling and extensive volcanism (Vlaar et al., 1994; van Thienen et al., 2004), the scale and extent of which are related to the intensity of the delamination process. A large-scale lower crustal and (or) lithospheric delamination or sinking may get arrested at the 660 km discontinuity identified by this study, where crustal and lithospheric components would be melted (Lustrino, 2005) because the mantle transition zone (MTZ) is a potential water reservoir

Solid Earth Discuss., doi:10.5194/se-2017-17, 2017
Manuscript under review for journal Solid Earth
Discussion started: 22 March 2017

Solid Earth
Discussions
Open Access

in the Earth's interior (Karato, 2011; Kuritani et al., 2011). Accumulation of subducted crustal debris, and delaminated crust and (or) lithosphere at the MTZ are speculated to give rise to 'second continents' on the bottom of the upper mantle (Kawai et al., 2013; Korenaga, 2004, Lustrino, 2005). The minerals in Earth's mantle transition zone as 'water tanks' might trigger dehydration melting of vertically flowing mantle (Schmandt et al., 2014). Because of their buoyancy, crustal and (or) lithospheric melts rise up as plume-like upwelling instead of being dragged down to the convecting lower mantle (Lustrino, 2005). Thus, lower crustal delamination and mantle inflow are considered to set the ideal scene for plume-like upwelling from the MTZ (He et al., 2014). Eventually, the plume-like upwelling resulted in the Emeishan LIP formation.

Meanwhile, removal of the lower crust and (or) lithosphere allows mantle to rise to shallower depths leading to decompression melting reflected as low velocity perturbations (Schott and Schmeling, 1998; Elkins-Tanton and Hager, 2000; Elkins-Tanton, 2005). Accordingly, some low velocity perturbations identified by this study may be the vestige of the mantle upwelling.

Conclusions

The tectonic framework of Emeishan LIP is characterized by the Longmenshan thrust fault in the northwest and the Ailaoshan-Red River strike slip fault in the southwest. It is possible that the assembly of Yangtze block with another crustal block in the Late Permian and Early Triassic might have led to crustal thickening and large-scale

Solid Earth Discuss., doi:10.5194/se-2017-17, 2017
Manuscript under review for journal Solid Earth
Discussion started: 22 March 2017

delamination of the lower crust and (or) lithosphere. The delamination resulted in the upwelling asthenosphere and generation of crustal melts that triggered plume-like upwelling and Emeishan LIP formation, with no evidence for any large plume rising from the CMB beneath the Emeishan LIP.

Acknowledgements

Waveform data for this study are provided by Data Management Centre of China National Seismic Network at Institute of Geophysics (SEISDMC, doi:10.11998/SeisDmc/SN), China Earthquake Networks Center and CQ, GX, GZ, QH, SC, XZ, YN Seismic Networks, China Earthquake Administration (Zheng et al., 2010). This study also contributes to the Foreign Expert funding from China University of Geosciences Beijing, and Professorial support from University of Adelaide to M. Santosh.

References

Ali, J.R., Fitton, J.G., Herzberg, C., 2010. Emeishan large igneous province (SW China) and the mantle-plume up-doming hypothesis: Journal of the Geological Society 167, 953–959.

Ali, J.R., Thompson, G.M., Zhou, M.F., Song, X.Y., 2005. Emeishan large igneous province, SW China. Lithos 79, 475– 489.

Anderson, D.L., 2007. Discussion of The Eclogite Engine: Chemical geodynamics as a

Galileo thermometer. GSA Special Papers 430, 47-64, doi: 10.1130/2007.2430(03).

Arndt, N., 2000. Hot heads and cold tails. Nature 407, 458-461.

Bai, Z.M., Tian, X.B., Tian, Y., 2011. Upper mantle P-wave tomography across the Longmenshan fault belt from passive-source seismic observations along Aba-Longquanshan profile. Journal of Asian Earth Sciences 40, 873–882.

Bao, X.W., Song, X.D., Li, J.T., 2015. High-resolution lithospheric structure beneath Mainland China from ambient noise and earthquake surface-wave tomography. Earth and Planetary Science Letters 417, 132–141.

Bryan, S.E., Ernst, R.E., 2008. Revised definition of Large Igneous Provinces (LIPs). Earth-Science Reviews 86, 175–202.

Buiter, S., 2014. How plumes help to break plates. Nature 513, 36-37.

Campbell, I.H., Griffiths, R.W., 1990. Implications of mantle plume structure for the evolution of flood basalts. Earthand Planetary Science Letters 99, 79-93.

Chung, S.L., Jahn, B.M., 1995. Plume-lithosphere interaction in generation of the Emeishan flood basalts at the Permian-Triassic boundary. Geology 23, 889–892.

Coffin, M.F., Eldholm, O., 2001. Large igneous provinces: progenitors of some ophiolites. In: Ernst, R.E., Buchan, K.L. (Eds.), Mantle Plumes: Their Identification through Time. : Special Paper, 352. Geological Society of America, pp. 59–70.

Data Management Centre of China National Seismic Network. Waveform data of China National Seismic Network. Institute of Geophysics, China Earthquake Administration, 2007, doi:10.11998/SeisDmc/SN, http://www.seisdmc.ac.cn.

Deng, J., Wang, Q.F., Yang, S.J., Liu, X.F., Zhang, Q.Z., Yang, L.Q., Yang, Y.H., 2010.

Solid Earth Discuss., doi:10.5194/se-2017-17, 2017
Manuscript under review for journal Solid Earth
Discussion started: 22 March 2017

Genetic relationship between the Emeishan plume and the bauxite deposits in Western Guangxi, China: Constraints from U–Pb and Lu–Hf isotopes of the detrital zircons in bauxite ores. Journal of Asian Earth Sciences 37, 412–424.

Dobretsov, N.L., 2011. Early Paleozoic tectonics and geodynamics of Central Asia: a role of mantle plumes. Russian Geology and Geophysics 52, 1539–1552.

Elkins-Tanton, L.T., 2005. Continental magmatism caused by lithospheric delamination. GSA Special Papers 388, 449-461.

Elkins-Tanton, L. T., Hager, B. H., 2000. Melt intrusion as a trigger for lithospheric foundering and the eruption of the Siberian flood basalts. Geophysical Research Letters 27, 3937–-3940.

Enkin, R.J., Yang, Z., Chen, Y., Courtillot, V., 1992. Paleomagnetic constraints on the geodynamic history of the major blocks of China from the Permian to the present. J. Geophys. Res. 97, 13953– 13989.

Ernst, R.E., Buchan, K.L., 2001. Large mafic magmatic events through time and links to mantle plume heads. Geological Society of America Special Paper 352, 483–576.

Ferris, A., Abers, G.A., Christensen, D.H., Veenstra, E., 2003. High-resolution mantle tomography of China and surrounding regions. Earth and Planetary Science Letters 214, 575-588.

Gao, S., Ling, W.L., Qiu, Y.M., Zhou, L., Hartmann, G., Simon, K., 1999. Contrasting geochemical and Sm-Nd isotopic compositions of Archean metasediments from the Kongling high-grade terrane of the Yangtze craton: evidence for cratonic evolution and redistribution of REE during crustal anatomies. Geochimica et Cosmochimica

Solid Earth Discuss., doi:10.5194/se-2017-17, 2017
Manuscript under review for journal Solid Earth
Discussion started: 22 March 2017

Acta, 63, 2071-2088.

Griffiths, R.W., Campbell, I.H., 1990. Stirring and structure in mantle starting plumes. Earth and Planetary Science Letters 99, 66–78.

Hales, T.C., Abt, D.L., Humphreys, E.D., Roering, J.J., 2005. A lithospheric instability origin for Columbia River flood basalts and Wallowa Mountains uplift in northeast Oregon. Nature 438, 843-845.

He, B., Xu, Y.G., Huang, X.L., Lou, Z.Y., Shi, Y.R., Yang, Q.J., Yu, S.Y., 2007. Age and duration of the Emeishan flood volcanism, SW China: Geochemistry and SHRIMP zircon U–Pb dating of silicic ignimbrites, post-volcanic Xuanwei Formation and clay tuff at the Chaotian section: Earth and Planetary Science Letters 255, 306–323.

He C.S., Zhu, L., Wang, Q.C., 2009. The significance of crust structure and continental dynamics inferred from receiver function in West Yunnan. Acta Geologica Sinca 83, 1163-1173.

He C.S., 2011. Seismic evidence for plume and subducting slab in West Yunnan, Southwestern China. Acta Geologica Sinca 85, 629-636.

He, C.S., Santosh, M., Wu, J.P., Chen, X.H., 2014e. Plume or no plume: Emeishan Large Igneous Province in Southwest China revisited from receiver function analysis. Physics of the Earth and Planetary Interiors 232, 72-78.

Herzberg, C., Asimow, P.D., 2008. Petrology of some oceanic island basalts: PRIMELT2.XLS software for primary magma calculation. Geochemistry, Geophysics, Geosystems 9. http://dx.doi.org/10.1029/2008GC002057.

Hofmann, A.W., 1997. Mantle geochemistry: the message from oceanic volcanism.

Solid Earth Discuss., doi:10.5194/se-2017-17, 2017
Manuscript under review for journal Solid Earth
Discussion started: 22 March 2017

Nature 385, 219–229.

Huang, K., Opdyke, N.D., 1998. Magnetostratigraphic investigations of an Emeishan basalt section in western Guizhou Province, China: Earth and Planetary Science Letters 163, 1-14.

Huang, R.Q., Wang, Z., Pei, S.P., Wang, Y.S., 2009. Crustal ductile flow and its contribution to tectonic stress in Southwest China. Tectonophysics 473, 476–489.

Huang, Z.C., Wang, P., Xu, M.J., Wang, L.S., Ding, Z.F., Wu, Y., Xu, M.J., Mi, N., Yu, D.Y., Li, H.,2015. Mantle structure and dynamics beneath SE Tibet revealed by new seismic images. Earth and Planetary Science Letters 411, 100–111.

Jiang, G.M., Zhao, D.P., Zhang, G.B., 2009. Crustal correction in teleseismic tomography and its application. Chinese J. Geophys. 52, 1508-1514.

Karato, S., 2011. Water distribution across the mantle transition zone and its implications for global material circulation. Earth and Planetary Science Letters 301, 413-423.

Kawai, K., Yamammoto, S., Tsuchiya, T., Maruyama, S., 2013. The second continent: Existence of granitic continental materials around the bottom of the mantle transition zone. Geoscience Frontiers 4, 1-6.

Kogiso, T., Hirschmann, M.M., Petermann, M., 2004. Highpressure partial melting of mafic lithologies in the mantle. J. Petrol. 45, 2407– 2422.

Kuritani, T., Ohtani, E., Kimura, J.I., 2011. Intensive hydration of the mantle transition zone beneath China caused by ancient slab stagnation. Nature Geoscience 4, 713-716.

Lei, J., Li, Y., Xie, F., Teng, J., Zhang, G., Sun, C., Zha, X., 2014. Pn anisotropic

Solid Earth Discuss., doi:10.5194/se-2017-17, 2017
Manuscript under review for journal Solid Earth
Discussion started: 22 March 2017

tomography and dynamics under eastern Tibetan plateau, J. Geophys. Res. Solid Earth, 119, 2174–2198, doi:10.1002/2013JB010847.

Li, C., van der Hilst, R.D., Toksöz, M.N., 2006. Constraining P-wave velocity variations in the upper mantle beneath Southeast Asia. Physics of the Earth and Planetary Interiors 154, 180–195.

Li, H.Y., Su, W., Wang, C.Y., Huang, Z.X., Lv, Z.Y., 2010. Ambient noise Love wave tomography in the eastern margin of the Tibetan plateau. Tectonophysics 491, 194–204.

Li, H.Y., Su, W., Wang, C.Y., Huang, Z.X., 2009. Ambient noise Rayleigh wave tomography in western Sichuan and eastern Tibet. Earth and Planetary Science Letters 282, 201–211.

Li, X.H., Li, Z.X., Zhou, H., Liu, Y., Kinny, P.D., 2002. U-Pb zircon geochronology, geochemistry and Nd isotopic study of Neoproterozoic bimodal volcanic rocks in the Kangdian rift of South China: implications for the initial rifting of Rodinia. Precambrian Research, 113, 135-154.

Li, Z., Li, X., Zhou, H., Kinny, P.D., 2002. Grenvillian continental collision in south China: new SHRIMP U-Pb zircon results and implications for the configuration of Rodinia. Geology 30, 163–166.

Li, Z.W., Ni, S.D., Roecker, S., 2014. Interstation Pg and Sg differential traveltime tomography in the northeastern margin of the Tibetan plateau: Implications for spatial extent of crustal flow and segmentation of the Longmenshan fault zone. Physics of the Earth and Planetary Interiors 227, 30–40.

Solid Earth Discuss., doi:10.5194/se-2017-17, 2017
Manuscript under review for journal Solid Earth
Discussion started: 22 March 2017

Lin, G., Li, X., Li, W., 2007. SHRIMP U-Pb zircon age, geochemistry and Nd-Hf isotope of Neoproterozoic mafic dyke swarms in western Sichuan: petrogenesis and tectonic significance. Science in China: Earth Sciences, 50, 1-16.

Liu, X., Gao, S., Diwu, C., Ling, W., 2008. Precambrian crustal growth of Yangtze craton as revealed by detrital zircon studies. American Journal of Science 308, 421-468.

Lü, Y., Zhang, Z.J., Pei, S.P., Sandvol, E., Xu, T., Liang, X.F., 2014 2.5-Dimensional tomography of uppermost mantle beneath Sichuan–Yunnan and surrounding regions. Tectonophysics 627, 193–204.

Lustrino, M., 2005. How the delamination and detachment of lower crust can influence basaltic magmatism: Earth-Science Reviews 72, 21–38.

Mao, J., Yangbo, C., Maohong, C., Pirajno, F., 2013. Major types and time–space distribution of Mesozoic ore deposits in South China and their geodynamic settings. Mineralium Deposita 48, 267-294.

Morgan, W.J., 1971. Convection plumes in the lower mantle. Nature 230, 42–43.

Paige, C., Saunders, M., 1982. LSQR: An algorithm for sparse linear equations and sparse least squares, Trans. Math. Software 8, 43–71, doi: 10.1145/355984.355989.

Pang, K.N., Zhou, M.f., Qi, L., Chung, S.L., Chu, C.H., Lee, H.Y., 2013. Petrology and geochemistry at the lower zone – Middle zone transition of the Panzhihua intrusion, SW China: Implications for differentiation and oxide ore genesis. Geoscience Frontiers 4, 517-533.

Peate, I.U., Bryan, S.E., 2008. Re-evaluating plume-induced uplift in the Emeishan large igneous province. Nature Geoscience 1, 625-629.

Solid Earth Discuss., doi:10.5194/se-2017-17, 2017
Manuscript under review for journal Solid Earth
Discussion started: 22 March 2017

Pirajno, F., 2007. Ancient to modern earth: the role of mantle plume in the making of continental crust: Earth's Oldest Rocks. Developments in Precambrian Geology, Kranendonk, M.J.V., Smithies, R.H., Bennett, V.C. (eds). 15, DOI: 10.1016/S0166-2635(07)15083-0.

Pirajno, F., 2007. Ancien to Modern Earth: The Role of Mantle Plumes in the Making of Continental Crust. Earth's Oldest Rocks Edited by Martin J. Van Kranendonk, R. Hugh Smithies and Vickie C. Bennett Developments in Precambrian Geology, Vol. 15 (K.C. Condie, Series Editor)

Pirajno, F., Hoatson, D.M., 2012. A review of Australia's Large Igneous Provinces and associated mineral systems: Implications for mantle dynamics through geological time. Ore Geology Reviews 48, 2–54.

Qiu, Y.M., Gao, S., McNaughton, N.J., Groves, D.I., Ling, W., 2000. First evidence of > 3.2 Ga continental crust in the Yangtze craton of south China and its implications for Archean crustal evolution and Phanerozoic tectonics. Geology, 28, 11-14.

Richards, M.A., Duncan, R.A., Courtillot, V.E., 1989. Flood basalts and hot-spot tracks; plume heads and tails. Science 246, 103-107.

Safonova, I.Y., Santosh, M., 2014. Accretionary complexes in the Asia-Pacific region: Tracing archives of ocean plate stratigraphy and tracking mantle plumes. Gondwana Research 25, 126-158.

Safonova, I.Y., Utsunomiya, A., Kojima, S., Nakae, S., Koizumi, K., Tomurtogoo, O., Filippov, A.N., 2009. Pacific superplume-related oceanic basalts hosted by accretionary complexes of Central Asia, Russian Far East and Japan. Gondwana

Solid Earth Discuss., doi:10.5194/se-2017-17, 2017
Manuscript under review for journal Solid Earth
Discussion started: 22 March 2017

Research 16, 587–608.

Schmandt, B., Jacobsen, S.D., Becker, T.W., Liu, Z., Dueker, K.G., 2014. Dehydration melting at the top of the lower mantle. Science 344, 1265-1268.

Sheth, H.C., 2007b. Plume-related regional pre-volcanic uplift in the Deccan Traps: Absence of evidence, evidence of absence. *GSA Spec. Pap.* 430, 785–814.

Sheth, H.C., 2007a. 'Large igneous provinces (LIPs)': definition, recommended terminology, and a hierarchial classification. Earth-Science Reviews 85, 117–124.

Shellnut, J.G., 2013. The Emeishan large igneous province: A synthesis. Geoscience Frontiers, http://dx.doi.org/10.1016/j.gsf.2013.07.003.

Shellnutt, J.G., 2014. The Emeishan large igneous province: a synthesis. Geoscience Frontiers, 5, 369-394.

Shellnutt, J.G., Iizuka, Y., 2012. Oxidation zonation within the Emeishan large igneous province: Evidence from mantle-derived syenitic plutons. Journal of Asian Earth Sciences 54–55, 31–40.

Shi, G.R., Shen, Z.S., 1998. A Changshingian (Late Permian) brachiopod fauna from Son La, northwest Vietnam. J. Asian Earth Sci. 16, 501– 511.

Smith, P.M., Asimow, P.D., 2005. Adiabat_1ph: a new public front-end to the MELTS, pMELTS, and pHMELTS models. Geochemistry, Geophysics, Geosystems 6, http://dx.doi.org/10.1029/2004GC000816.

Song, H.J. Wignall, P.B., Tong, J.N., Yin, H.F., 2013. Two pulses of extinction during the Permian–Triassic crisis. Nature Geoscience 6, 52-56.

Song, X.Y., Zhou, M.F., Cao, Z.M., Robinson, P.T., 2004. Late Permian rifting of the

Solid Earth Discuss., doi:10.5194/se-2017-17, 2017
Manuscript under review for journal Solid Earth
Discussion started: 22 March 2017

Solid Earth Discussions

South China Craton caused by the Emeishan mantle plume?. Journal of the Geological Society, London, 161, 773–781.

Sun, S.S., Ji, S.C., Wang, Q., Wang, H.C, Long, C.X, Salisbury, M., 2012. Seismic properties of the Longmen Shan complex: Implications for the moment magnitude of the great 2008 Wenchuan earthquake in China. Tectonophysics 564–565, 68–82.

Tang, Q., Li, C., Zhang, M., Lin, Y., 2015. U-Pb age and Hf isotopes of zircon from basaltic andesite and geochemical fingerprinting of the associated picrites in the Emeishan large igneous province, SW China. Mineralogy and Petrology 109, 103-114.

Tien, C.P., 2000. The Permian of Vietnam, Laos and Cambodia and its interregional correlation. In: Yin, H., Dickins, J.M., Shi, G.R., Tong, J. (Eds.), Permo-Triassic Evolution of Tethys and Western Circum-Pacific. Elsevier, pp. 99–109.

Uenzelmann-Neben, G., 2013. Magma giant. Nature Geoscience 6, 902-903.

Ukstins Peate, I., Bryan, S.E., 2008. Re-evaluating plume-induced uplift in the Emeishan large igneous province. Nature Geoscience, 1, 625–629.

Usuki, T., Lan, C.Y., Hoa, T.T., Dung, P.T., Wang, K.-L., Shellnutt, J.G., Chung, S.-L., 2015. Zircon U-Pb ages and Hf isotopic compositions of alkaline silicic magmatic rocks in the Phan Si Pan-Tu Le region, northern Vietnam: identification of a displacement western extension of the Emeishan large igneous province. Journal of Asian Earth Sciences 97, 102-124.

van Thienen, P., van den Berg, A.P., Vlaar, N.J., 2004. Production and recycling of oceanic crust in the early Earth. Tectonophysics 386, 41–65.

Solid Earth Discuss., doi:10.5194/se-2017-17, 2017
Manuscript under review for journal Solid Earth
Discussion started: 22 March 2017

Vlaar, N.J., van Keken, P.E., van den Berg, A.P., 1994. Cooling of the Earth in the Archaean: consequences of pressure-release melting in a hotter mantle. Earth and Planetary Science Letters 121, 1–18.

Wang, C.Y., Zhou, M.F., Qi, L., 2007. Permian flood basalts and mafic intrusions in the Jinping (SW China) – Song Da (northern Vietnam) district: Mantle sources, crustal contamination and sulfide segregation. Chemical Geology 243, 317 – 343.Wang, Y., Santosh, M., Luo, Z.H., Hao, J.H., 2015. Large igneous provinces linked to supercontinent assembly. Journal of Geodynamics 85, 1–10.

White, W.M., 2010. Oceanic island basalts and mantle plumes: the geochemical perspective. Annual Review of Earth and Planetary Sciences 38, 133–160.

Wignall, P.B., 2011. Lethal volcanism. Nature 477, 285-286.

Wilson, J.T., 1963. A possible origin of the Hawaiian Islands. Canadian Journal of Physics 41, 863–870.

Xiao, L., Xu, Y.G., Mei, H.J., Zheng, Y.F., He, B., Pirajno, F., 2004. Distinct mantle sources of low-Ti and high-Ti basalts from the western Emeishan large igneous province, SW China: implications for plume–lithosphere interaction: Earth and Planetary Science Letters 228, 525– 546.

Xu, L.L., Rondenay, S., van der Hilst, R.D., 2007. Structure of the crust beneath the southeastern Tibetan Plateau from teleseismic receiver functions. Physics of the Earth and Planetary Interiors 165, 176–193.

Xu, Y.G., He, B., Chung, S.L., Menzies, M., Frey, F.A., 2004. Geologic, geochemical, and geophysical consequences of plume involvement in the Emeishan flood-basalt

Solid Earth Discuss., doi:10.5194/se-2017-17, 2017
Manuscript under review for journal Solid Earth
Discussion started: 22 March 2017

province. Geology, 32, 917-920.

Xu, Y.G., He, B., Huang, X.L., Luo, Z.Y., Chung, S.L., Xiao, L., Zhu, D., Shao, H., Fan, W.M., Xu, J.F., Wang, Y.J., 2007. Identification of mantle plumes in the Emeishan Large Igneous Province. Episodes, Vol. 30, no. 1 32-42.

Xu, Y., Yang, X.T., Li, Z.W., Liu, J.H., 2012. Seismic structure of the Tengchong volcanic area southwest China from local earthquake tomography. Journal of Volcanology and Geothermal Research 239–240, 83–91.

Xu, Y.G., Chung, S.L., Jahn, B.M., Wu, G.Y., 2001. Petrologic and geochemical constraints on the petrogenesis of Permian–Triassic Emeishan flood basalts in Southwestern China. Lithos 58, 145–168.

Yang, T., Wu, J.P., Wang, W.L., 2014. Complex Structure beneath the Southeastern Tibetan Plateau from Teleseismic P-Wave Tomography. Bulletin of the Seismological Society of America 104, 1056–1069.

Zheng X F, Yao Z X, Liang J H, Zheng J. The role played and opportunities provided by IGP DMC of China National Seismic Network in Wenchuan earthquake disaster relief and researches. Bull. Seismol. Soc. Am., 2010, 100(5B) ： 2866~2872, doi: 10.1785/0120090257.

Zhao, D., 2004. Global tomographic images of mantle plumes and subducting slabs: Insight into deep Earth dynamics. Physics of the Earth Planetary Interiors 146, 3-34.

Zhao, D., Hasegawa, A., Horiuchi, S., 1992. Tomographic imaging of P and S wave velocity structure beneath northeastern Japan. J. Geophys. Res. 97, 19,909–19,928, doi: 10.1029/92JB00603.

Solid Earth Discuss., doi:10.5194/se-2017-17, 2017
Manuscript under review for journal Solid Earth
Discussion started: 22 March 2017

Zhao, D., Hasegawa, A., Kanamori, H., 1994. Deep structure of Japan subduction zone as derived from local, regional and teleseismic events. Journal of Geophysical Research 99, 22,313–22,329.

Zhao, D., Mishra, O., Sanda, R., 2002. Influence of fluids and magma on earthquakes: Seismological evidence. Phys. Earth Planet. In. 132,249–267, doi: 10.1016/S0031-9201(02)00082-1. Zheng, X.F., Yao, Z.X., Liang, J.H., Zheng, J., 2010. The Role Played and Opportunities Provided by IGP DMC of China National Seismic Network in Wenchuan earthquake disaster relief and researches. Bull. Seism. Soc. Am. 100(5B), 2866-2872.

Zhao, D., Ohtani, E., 2009. Deep slab subduction and dehydration and their geodynamic consequences: evidence from seismology and mineral physics, Gondwana Res. 16, 401–413.

Zhao, D., Xu, Y.B., Wiens, D.A., Dorman, L., Hildebrand, J., Webb, S., 1997. Depth extent of the Lau back-arc spreading center and its relation to subduction processes. Science 278, 254–257.

Zhao, D., Tian, Y., Lei, J., Liu, L., Zheng, S., 2009. Seismic image and origin of the Changbai intraplate volcano in East Asia: Role of big mantle wedge above the stagnant Pacific slab. Phys. Earth Planet. Inter. 173, 197-206.

Zhao, D., Yamamoto, Y., Yanada, T., 2013. Global mantle heterogeneity and its influence on teleseismic regional tomography. Gondwana Res. 23, 595–616.

Zhao, D., 2001. Seismic structure and origin of hotspots and mantle plumes. Earth and Planetary Science Letters 192, 251– 265.

Zhao, D., 2004. Global tomographic images of mantle plumes and subducting slabs: Insight into deep Earth dynamics. Physics of the Earth Planetary Interiors 146, 3-34.

Zhao, D., Hasegawa, A., Horiuchi, S., 1992. Tomographic imaging of P and S wave velocity structure beneath northeastern Japan. J. Geophys. Res. 97, 19,909–19,928, doi: 10.1029/92JB00603.

Zhao, D., Hasegawa, A., Kanamori, H., 1994. Deep structure of Japan subduction zone as derived from local, regional and teleseismic events. Journal of Geophysical Research 99, 22,313–22,329.

Zhao, D., Mishra, O., Sanda, R., 2002. Influence of fluids and magma on earthquakes: Seismological evidence. Physics of Earth Planetary letters. 132,249–267, doi: 10.1016/S0031-9201(02)00082-1.

Zheng, Y.F., Xiao, W.J., Zhao, G.C., 2013. Introduction to tectonics of China. Gondwana Research 23, 1189–1206.

Zhong, H., Zhu, W.G., Hu, R.Z., Xie, L.W., He, D.F., Liu, F., Chu, Z.Y., 2009. Zircon U-Pb age and Sr-Nd-Hf isotope geochemistry of the Panzhihua A-type syenitic intrusions in the Emeishan large igneous province, southwest China and implications for growth of juvenile crust. Lithos 2009, 109-128.

Zhou, M.F., Chen, W.T., Wang, C.Y., Prevec, S.A., Liu, P.P., Howarth, G.F., 2013. Two stages of immiscible liquid separation in the formation of Panzhihua-type Fe-Ti oxide deposits, SW China. Geoscience Frontiers 4, 481-502.

Zhou, X., Zhu, Y., 1993. Late Proterozoic collisional orogen and geosuture in southeastern China: petrological evidence. Chinese Journal of Geochemistry 12, 239–251.

Solid Earth Discuss., doi:10.5194/se-2017-17, 2017
Manuscript under review for journal Solid Earth
Discussion started: 22 March 2017

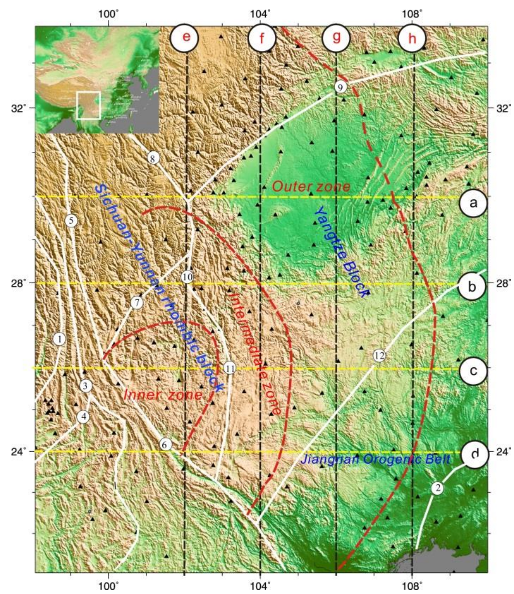

Fig. 1. Tectonic framework, distribution of seismic stations (black triangle) and the west-east and north-south direction profiles in the Emeishan LIP area. 1: Nujiang fault, 2: Shaoxing-Jiangshan-Pingxiang fault, 3: Langcangjiang fault, 4: Nandinghe fault, 5: Weixi-Qiaohou fault, 6: Honghe fault, 7: Yangjiang-Xiaojinhe fault, 8: Xianshuihe fault, 9: Longmenshan fault, 10: Anninghe-Zhemuhe fault, 11: Xiaojiang fault, 12: Jiujiang-Shitai buried fault, black triangle: seismic station.

Solid Earth Discuss., doi:10.5194/se-2017-17, 2017
Manuscript under review for journal Solid Earth
Discussion started: 22 March 2017

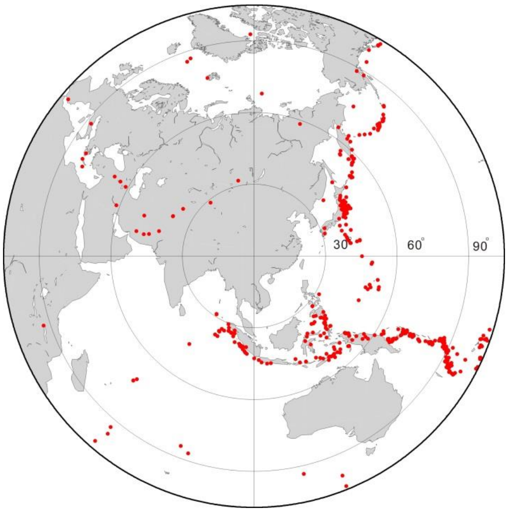

Fig. 2. Seismic events used in this tomographic study. The 371 events with epicenter distance range from 30 ° to 85 ° for each station-event pair.

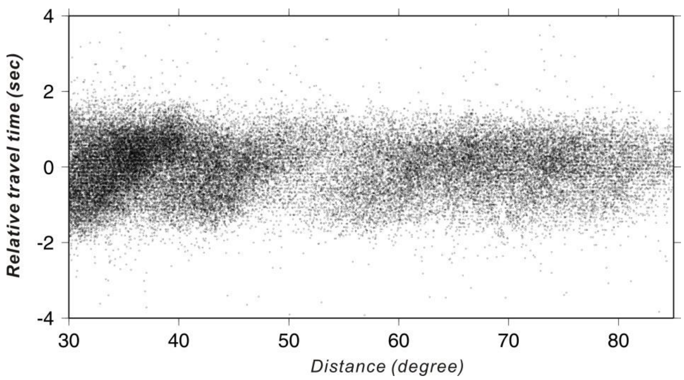

Fig. 3 Distribution of relative arrival time. We limited to >-2s and <2s for the tomographic inversion.

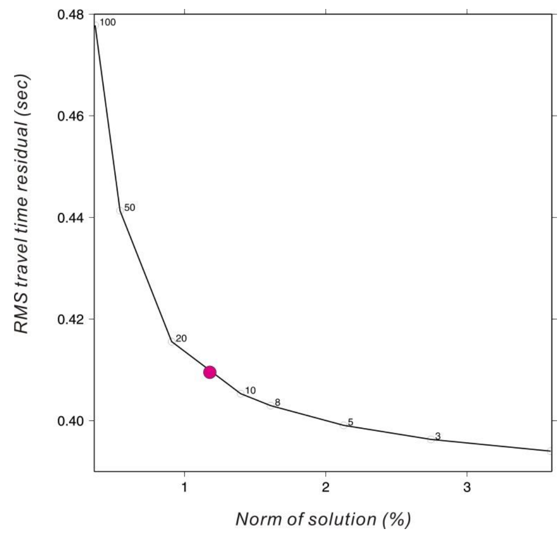

Fig. 4 The damping parameter (15) taken to invert final solution model (red circle) for CRT and synthethic tests after a series inversion test. RMS travel time residual is about 0.41 s.

Solid Earth Discuss., doi:10.5194/se-2017-17, 2017
Manuscript under review for journal Solid Earth
Discussion started: 22 March 2017

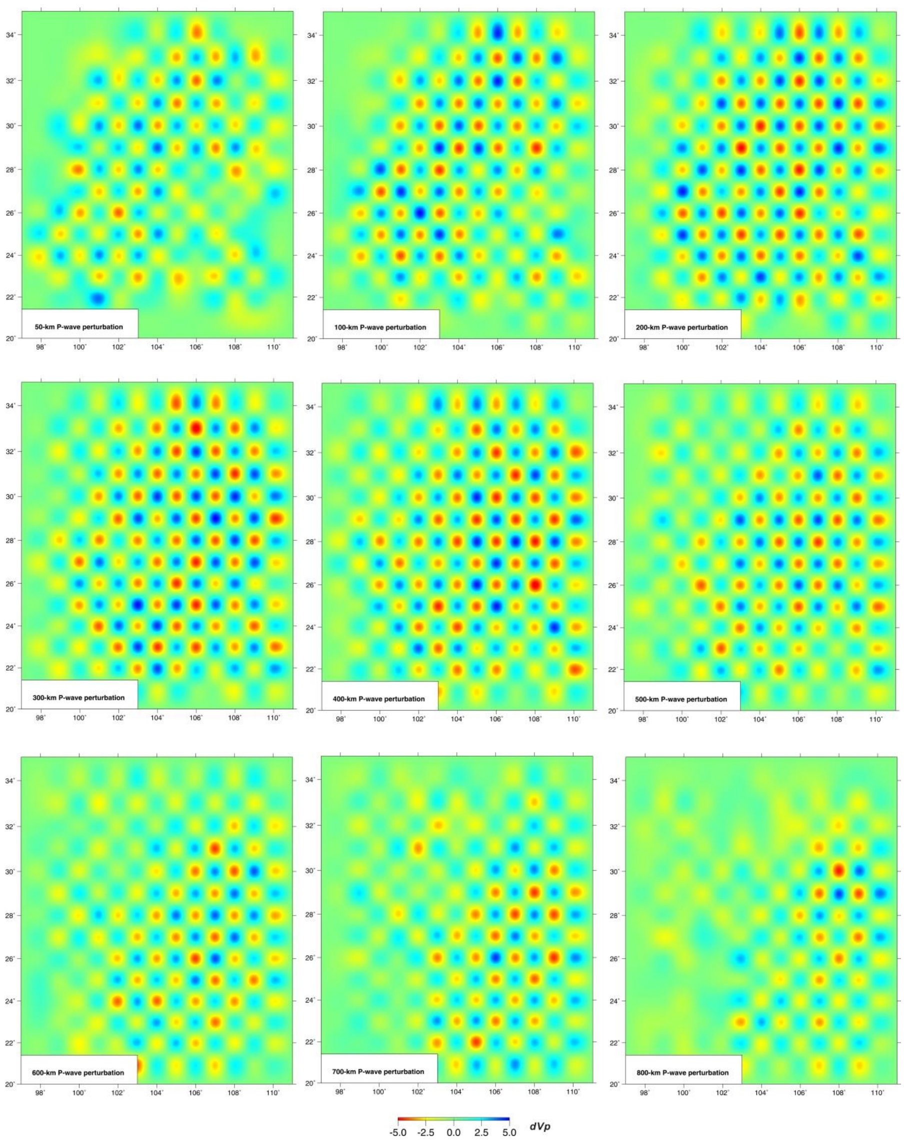

Fig.5 Checkboard resolution test at 50, 100, 200, 300, 400, 500, 600, 700 and 800 km depth sections relative to IASP91 1D velocity model (Kennett and Engdahl, 1991). The model was run using the same raypaths as the main inversion, with the same damping parameter.

Solid Earth Discuss., doi:10.5194/se-2017-17, 2017
Manuscript under review for journal Solid Earth
Discussion started: 22 March 2017

Solid Earth Discussions

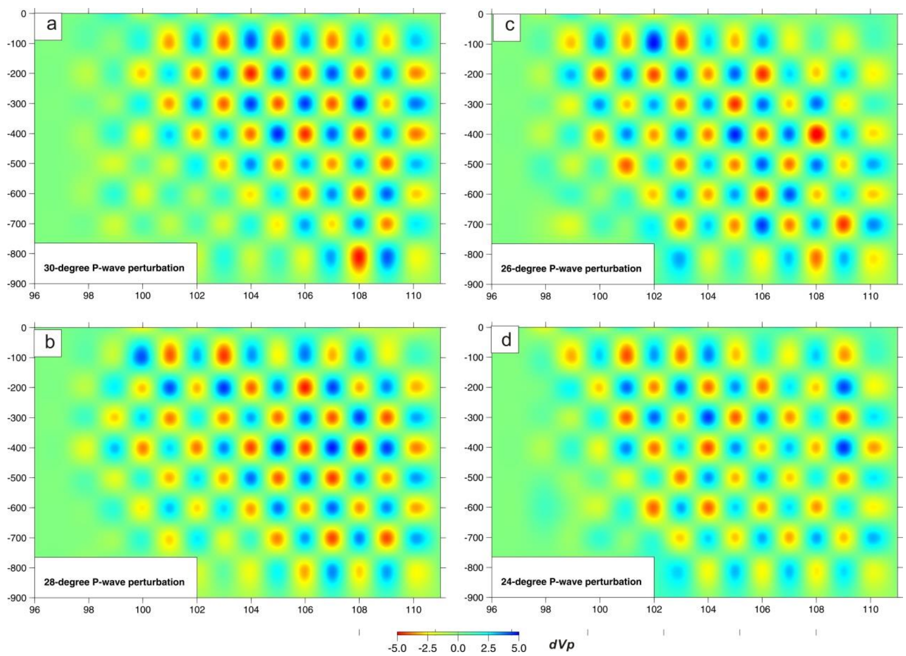

Fig. 6 Checkboard resolution test along the west-east direction profiles (a, b, c, and d is latitude 24° N, 26° N, 28° N and 30° N direction, respectively) (see Fig. 1 for profile location).

Solid Earth Discuss., doi:10.5194/se-2017-17, 2017
Manuscript under review for journal Solid Earth
Discussion started: 22 March 2017

Solid Earth
Discussions

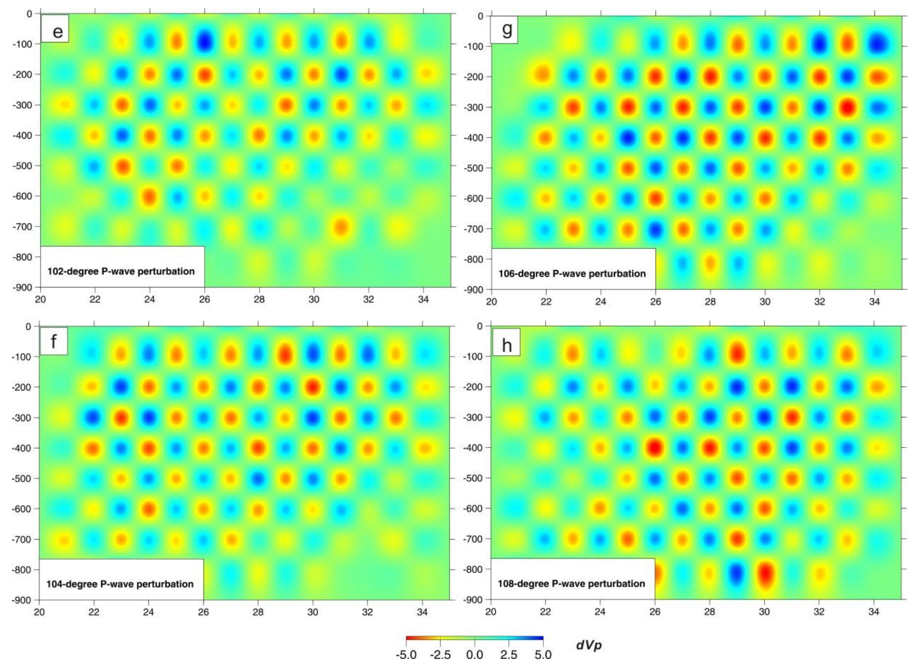

Fig. 7 Checkboard resolution test along the north-south direction profiles (e, f, g and h are sections along longitude 102° E, 104° E, 106° E and 108° E, respectively) (see Fig. 1 for profile location).

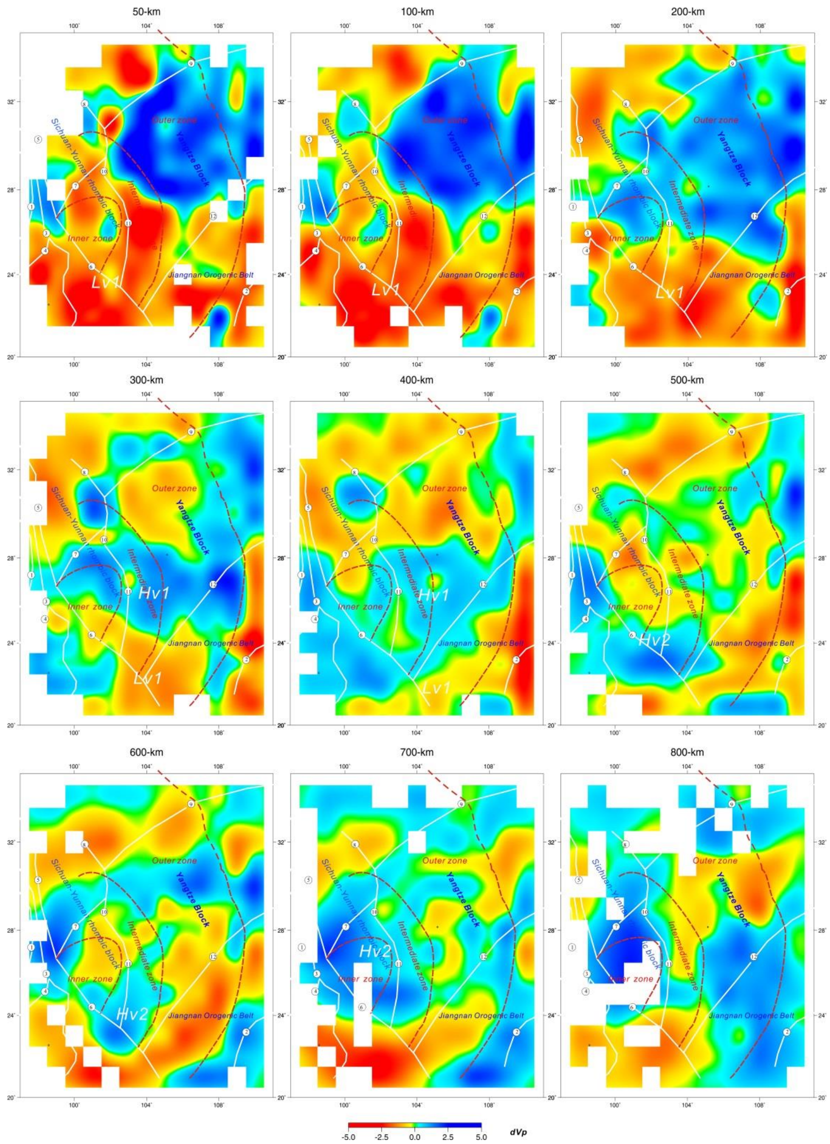

Fig. 8 P-wave velocity perturbation at 50, 100, 200, 300, 400, 500, 600, 700 and 800 km depth sections relative to IASP91 1D velocity model (Kennett and Engdahl, 1991). Portions of the model where the recovery of the starting model in the CRT was below 10% are not shown (see Fig. 5).

Solid Earth Discuss., doi:10.5194/se-2017-17, 2017
Manuscript under review for journal Solid Earth
Discussion started: 22 March 2017

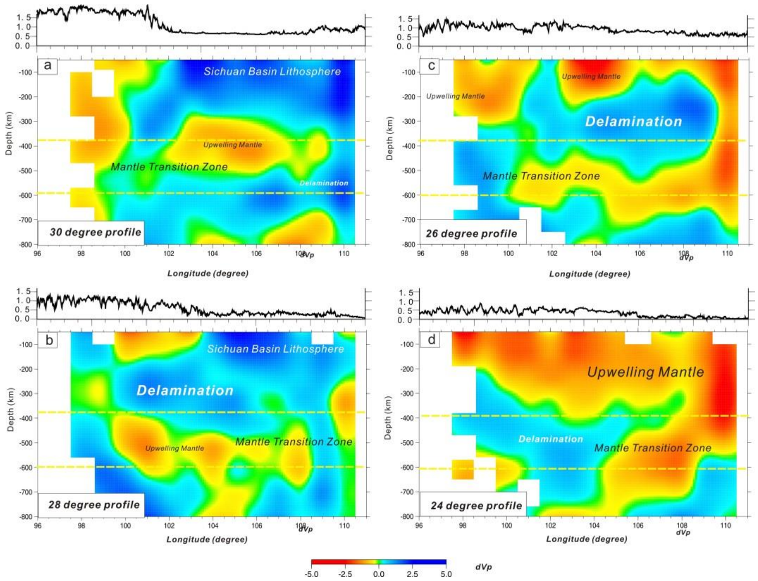

Fig. 9 P-wave velocity perturbation profiles along the west-east direction (a, b, c, and d is latitude 24° N, 26° N, 28° N and 30° N direction, respectively) (see Fig. 1 for profile location). Portions of the model where the recovery of the starting model in the CRT was below 10% are not shown (see Fig. 6).

Solid Earth Discuss., doi:10.5194/se-2017-17, 2017
Manuscript under review for journal Solid Earth
Discussion started: 22 March 2017

Solid Earth
Discussions
Open Access

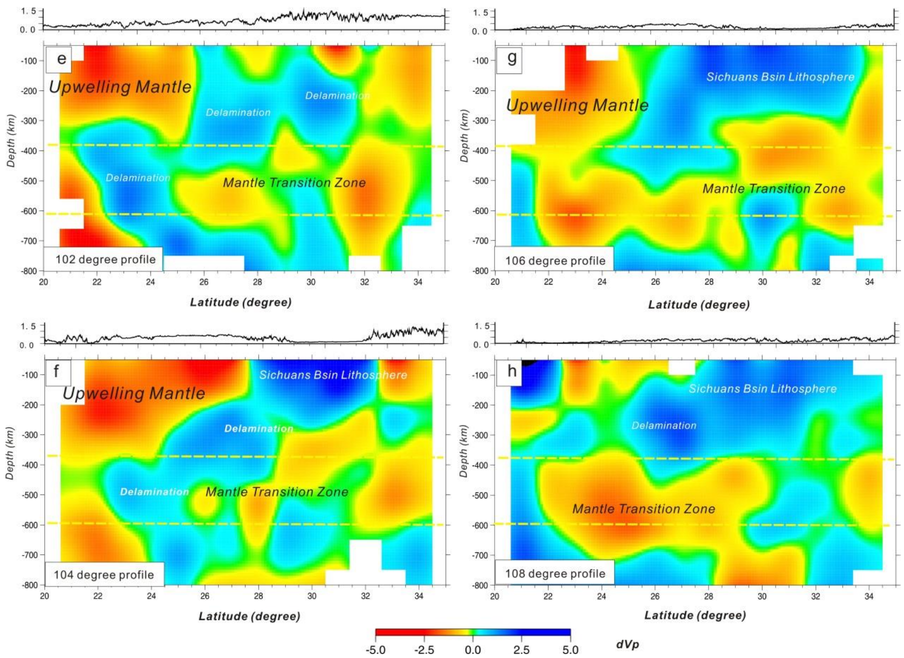

Fig. 10 P-wave perturbation profiles along the north-south direction (e, f, g and h are sections along longitude 102° E, 104° E, 106° E and 108° E, respectively) (see Fig. 1 for profile location). Portions of the model where the recovery of the starting model in the CRT was below 10% are not shown (see Fig. 7).